2025 IEEE International Conference on Systems, Man, and Cybernetics (SMC)
October 5-8, 2025. Vienna, Austria

2025 IEEE International Conference on Systems, Man, and Cybernetics (SMC) | 979-8-3315-3358-8/25/$31.00 ©2025 IEEE | DOI: 10.1109/SMC58881.2025.11342576

Predicting Human Detection of Changes in Controlled Element Dynamics in Manual Control

Thomas Eppenga, Daan M. Pool, Marinus M. van Paassen and Max Mulder

***Abstract*— A pursuit-tracking manual control model is introduced that includes an observer-like internal model to predict human detection of a change in controlled element dynamics. The internal model's innovation signal, the difference between the observed and expected system response, is studied for its capacity to drive the detection of a change. The model's performance is tested for different crossover frequencies, remnant power ratios, observer gains, and detection threshold settings, through Monte Carlo analysis of simulated pursuit-tracking tasks where the controlled element transitions from single to double integrator dynamics. The model shows highly accurate detection performance for a wide range in the observer gain, with a true positive rate of approximately 1 and a false positive rate of approximately 0.02. The high true and low false positive rates, combined with average detection times that match experimental human-in-the-loop data, show the observer model's potential for accurately predicting human detection of a change in controlled element dynamics.**

I. Introduction

Understanding the unique human capability to quickly adapt their control strategy in unexpected events, is essential to further advance automation, human training and support systems [1]. Young [2] summarizes research on the adaptive Human Controller (HC), identifying three process phases: *detection*, *identification*, and *modification*. He also identified four types of adaptation, to input patterns, Controlled Element (CE) dynamics, task adaptation, and programmed adaptation. This paper focuses on the HC detection phase, in adapting to changing CE dynamics. In line with recent work [1], [3]–[5], pursuit tracking is studied, with the CE dynamics changing from single integrator-like (SI) to double integrator-like (DI) dynamics.

Inspired by Adaptive Model Theory (AMT) [6], [7], here we propose a HC detection model based on an internally-generated *innovation* signal [4]. The innovation is the difference between the expected CE output, based on an internal model of the CE dynamics and the current input to the CE, and the perceived CE output. When this signal, processed by an observer, exceeds some internally stored threshold, calibrated during extensively tracking a non-varying CE, the HC is assumed to detect a change in the CE dynamics.

This paper discusses the feasibility of this model. A Monte Carlo (MC) simulation analysis was performed, varying crucial HC parameters such as crossover frequency, remnant power ratio, the observer gain, and threshold values from 1σ to 10σ of the analytically-obtained innovation signal standard deviation (SD). Average detection times were compared with experimental data obtained by Barragan et al. [5].

Control & Simulation, Faculty of Aerospace Engineering, TU Delft, The Netherlands. Email: {d.m.pool, m.m.vanpaassen, m.mulder}@tudelft.nl

The paper is structured as follows. Section II summarizes literature and the proposed detection method. Section III presents the Monte Carlo simulation analysis and settings, the results of which are discussed in Section IV and Section V. The paper ends with conclusions, Section VI.

II. Background, detection model and scheme

A. Previous work

Whereas most previous studies in adaptive manual control applied a compensatory display [2], [8], [9], a pursuit display is used here, Fig. 1. On a pursuit display, an operator can see the system response to the applied control actions, $y(t)$, and compare it with the expected system response $f_t(t)$.

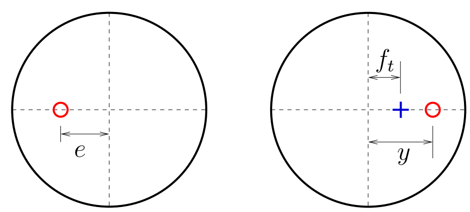

Fig. 1: Compensatory (left) and pursuit display (right).

The adaptive human manual control models studying compensatory tracking show a range of potential ways in which humans can detect changes in CE dynamics. Internal models, which check whether the difference between perceived versus expected error-*rate* $\dot{e}(t)$ exceeds a certain learned threshold value are dominant in literature [8]. Others explored the use of decision regions, boundaries based on stored variations in error $e(t)$ and error-rate $\dot{e}(t)$ in steady-state tracking, and again detecting a change when these boundaries are exceeded [9]. These decision regions are empirically determined, relying on specific system dynamics transitions. Van Ham et al. [10] replicated the work of [9] and proposed limits around 3.9σ of both the system error $e(t)$ and system error rate $\dot{e}(t)$.

These compensatory tracking models do not carry over well to pursuit tracking, where the operator is presented with the target signal $f_t(t)$ *and* the CE response $y(t)$ separately. Hess proposed an adaptive pilot model for pursuit tracking based on the definition of tracking criteria which, when exceeded, would indicate a change in CE dynamics [11]. Terenzi et al. investigated Model Reference Adaptive Control (MRAC), inspired by predictive coding in neuroscience [12].

Inspired by pioneering work on Adaptive Model Theory (AMT) [6], [7], Mulder et al. [4] proposed a comprehensive model of the human adaptive process in pursuit tracking.

Using an internal model of task variables, skilled HCs are hypothesized to be able to notice changes in these task variables when their expectation does not match their observation. That is, proficient HCs can infer the statistical characteristics of the target signal $f_t(t)$, disturbances affecting the system, and changes in the CE dynamics. The difference between the observation and expectation is the innovation signal $\eta(t)$. This model will be further studied in this paper.

B. Detection model

Fig. 2 illustrates a simplified version of the model, with $H_n(s)$ the remnant filter, $H_p(s)$ the HC model, $H_{nm}(s)$ neuromuscular and stick dynamics, $H_{CE}(s)$ the CE dynamics, $H^*_{CE}(s)$ the HC's internal model of the CE dynamics, K the observer gain and η the innovation signal.

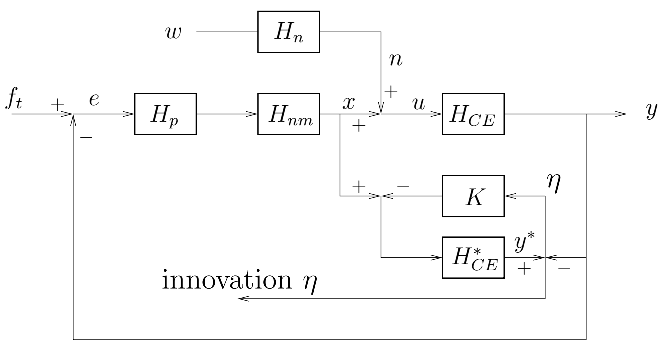

Fig. 2: Adapted Mulder et al. model [4], with observer added. In this figure, the (t) and (s) variables are omitted for brevity.

The closed-loop system has two inputs: the target signal $f_t(t)$ and the white noise $w(t)$ as input to the remnant filter. From Fig. 2 the innovation signal $\eta(t)$ can be derived as:

$$\mathcal{L}\{\eta\} = \frac{H_p H_{nm}(H_{CE} - H^*_{CE})}{(1 + H_p H_{nm} H_{CE})(1 + K H^*_{CE})} F_t + \frac{H_{CE}(1 + H_p H_{nm} H^*_{CE})}{(1 + H_p H_{nm} H_{CE})(1 + K H^*_{CE})} N \tag{1}$$

When the internal model matches the true CE dynamics, $H^*_{CE}(s) = H_{CE}(s)$, which is the case in steady-state tracking, i.e., when the CE dynamics do not change, then (1) becomes:

$$\mathcal{L}\{\eta\} = \frac{H_{CE}}{1 + K H_{CE}} N \tag{2}$$

This allows the innovation signal variance σ^2_η to be analytically computed. Eq. (2) shows that, also with constant CE dynamics the innovation signal $\eta(t)$ will be non-zero. In this case it is fully driven by the HC remnant, representing non-linear, time-varying effects of control behavior, *unknown* to the human controller [13]. The innovation reflects the differences between what an operator expects to see on the pursuit display, $y^*(t)$, based on the internal model of the CE dynamics and the input $u(t)$ given, and perceives from the display, $y(t)$. An experienced HC accepts some variation in the innovation because of remnant, even when the CE dynamics do not change. When this variation becomes too large (larger than 'normal'), however, the HC may conclude that 'something has changed' in the CE dynamics, the only task variable that can change in our study. Hence, the SD of the innovation signal in steady-state tracking, σ_η, is considered here as a potential threshold for detecting changes in CE dynamics. When the innovation signal magnitude exceeds some multiple C of this SD, $|\eta(t)| > \mathrm{C}\sigma_\eta$, the operator concludes that a change in CE dynamics occurs.

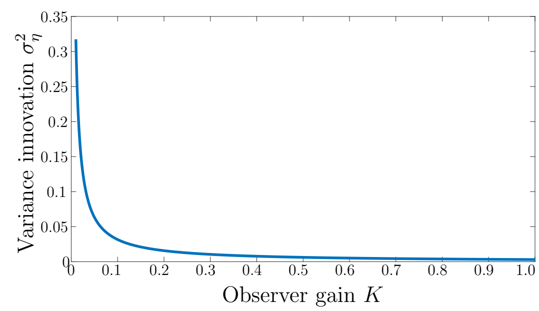

Fig. 3: Variance of innovation signal σ^2_η for HC observer model gains K ranging from 0.01 to 1.

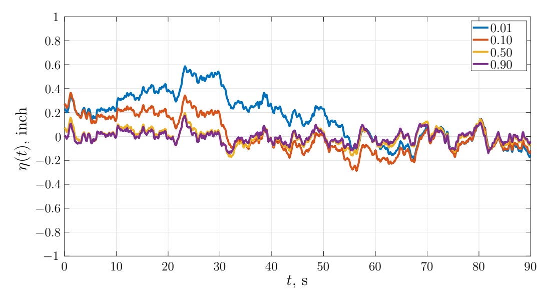

Fig. 4: Innovation realisations $\eta(t)$, for four observer gains K (see legend), HC gain 5.5, remnant power ratio 0.05.

The HC model includes an observer (gain K) that adjusts the internal model's system state using observations [14]. Fig. 3 shows the innovation variance, σ^2_η, for gains K between 0.01 and 1, for single integrator-like CE dynamics. For $K = 0$, (2) shows that $\eta(t)$ then equals the remnant $n(t)$ passed through the CE dynamics $H_{CE}(s)$, which results in a 'random walk': the innovation signal will on average be zero mean, its variance would be infinite for $t \to \infty$. Analytical bounds cannot be determined and the innovation $\eta(t)$ cannot be used to determine a change in CE dynamics. Fig. 4 shows four realisations of $\eta(t)$, for four observer gains K, computed with identical $f_t(t)$ and $w(t)$ inputs.

On the other hand, setting $K > 1$ would imply that the innovation is predominantly driven by observation rather than expectation, rendering the HC internal model ineffective, which is not supported by literature [5]. Therefore, observer gains greater than 0.9 are not considered, and only gains between 0.1 and 0.9 will be further evaluated in this paper.

C. Detection scheme

To obtain reasonable settings for the constant C and the observer gain K, Receiver Operating Characteristic (ROC) curves were used. An ROC curve plots the true positive (TP) rate (3) against the false positive (FP) rate (4):

$$\text{TP}_{\text{rate}} = \text{TP}/(\text{TP}+\text{FN}) \tag{3}$$

$$\text{FP}_{\text{rate}} = \text{FP}/(\text{FP}+\text{TN}) \tag{4}$$

with FN and TN false and true negative, respectively.

When a change in CE dynamics does *not* happen, and $|\eta(t)|$ exceeds the analytical threshold, an FP occurs. When $|\eta(t)|$ remains sub-threshold, a TN is counted.

When a change in CE dynamics does occur and $|\eta(t)|$ exceeds the threshold *after* the CE dynamics change, a TP occurs. When $|\eta(t)|$ remains sub-threshold *after* the CE dynamics change, an FN is counted. When $|\eta(t)|$ exceeds the threshold *before* the CE dynamics change, a FP is counted.

III. Method

A. Rationale

A Monte Carlo (MC) analysis was performed to study the effects of various settings of the simulated HC and observer model on the success and timing of detecting a CE dynamics change. The computer simulations were run for two HC gains K_p, three remnant power ratio settings P_n and twelve observer gains K. For each of the 72 combinations of these parameters, $3,000$ runs were done, all unique realisations.

For every realisation, two simulations are run, with identical $f_t(t)$ and $n(t)$: one without a CE change, and one with a change in CE dynamics. For each realisation, the (no CE change) FP or TN, or (CE change) TP, FP and FN were calculated for 10 multiples of C, as the threshold is defined as $\mathrm{C}\sigma_\eta$, to compute the TP and FP *rate* per observer gain.

ROC curves were constructed per remnant power ratio and HC gain, resulting in six different curves. Similarly, the detection *times* were computed for all these combinations. In the following, the MC settings will be briefly explained.

B. Controlled Element dynamics $H_{CE}(s)$

All runs started with single integrator-like CE dynamics. In half of the runs, the CE dynamics changed to double-integrator-like dynamics, at 95 seconds, according to:

$$H_{CE}(s,t) = K_{CE}(t)/s(s+\omega_b(t)) \tag{5}$$

with $K_{CE}(t)$ and $\omega_b(t)$ the (possibly) time-varying CE gain and break frequency [5], [12]. To simulate a change in CE dynamics, a sigmoid activation function was used:

$$P(t) = P_1 + (P_2 - P_1)/(1+e^{-G(t-\tau)}) \tag{6}$$

where P_1 and P_2 represent the initial and final parameter values, τ is the time of maximum rate of change and G is the maximum rate of change. G was set to 100 s^{-1}, which means that the CE dynamics change occurs in $\approx$0.1 s [5]. In the time-varying CE conditions, K_{CE} changed from 15 to 2 and ω_b from 20 to 0.2 rad/s [5], [12].

C. Target signal $f_t(t)$

The target signal was a sum of ten sinusoids:

$$f_t(t) = \sum_{n=1}^{10} A_t[n]\sin(k[n]\omega_m t + \phi_t[n]) \tag{7}$$

with $A_t[n]$ the amplitude, $k[n]\omega_m$ the frequency and $\phi_t[n]$ the phase of the n^{th} sinusoid. The signal $f_t(t)$ was crested to make sure that it was bounded in amplitude. To avoid spectral leakage, the fundamental frequency ω_m was set at $2\pi/T_m$, with T_m the measurement time (90 s). With a run-in time of 10 s, the total simulation time per run was 100 s.

TABLE I: Example of crested target signal parameters.

n (-)	$k[n]$ (-)	ω_t (rad/s)	ϕ_t (rad)	A_t (inch)
1	3	0.209	5.323	0.286
2	5	0.349	5.496	0.286
3	9	0.628	5.151	0.286
4	11	0.768	2.469	0.286
5	17	1.187	1.343	0.286
6	27	1.885	0.888	0.286
7	43	3.002	2.514	0.029
8	71	4.957	3.969	0.029
9	131	9.146	1.365	0.029
10	233	16.267	3.894	0.029

D. HC model $H_p(s)H_{nm}(s)$

The HC model was an extended 'simplified precision model' for compensatory tracking [13]:

$$H_p(s)H_{nm}(s) = K_p e^{-js\tau_e}\frac{\omega_{nm}^2}{\omega_{nm}^2 + 2\zeta_{nm}\omega_{nm}s + s^2} \tag{8}$$

This model can describe HC dynamics in pursuit tracking tasks as well when controlling single integrator-like CE dynamics [15]. Neuromuscular dynamics were fixed at $\omega_{nm} =$ 15 rad/s, and $\zeta_{nm} = 0.7$; the time delay τ_e was fixed at 0.09 s.

The HC gain was set at either 3.5 (low gain HC) or 5.5 (high gain), corresponding with crossover frequencies and phase margins of (2.6 rad/s, 55.1 deg) and (4 rad/s, 35.6 deg), respectively. These values correspond to experimental values [5] and reflect less or more aggressive human controllers.

Note that the HC dynamics did not change during the simulation, which means that in the simulation runs where the CE dynamics changed from single-integrator-like to double-integrator-like, the loop became unstable.

The internal model $H^*_{CE}(s)$ in the observer was always fixed and equal to the single integrator-like CE dynamics before transition. The observer gain K was varied from 0.01 to 0.9, in twelve steps (0.01, 0.025, 0.05, 0.1-0.9).

E. HC remnant model $H_n(s)$

Remnant $n(t)$ was simulated as filtered Gaussian white noise. For every realisation a unique remnant signal was created. The second-order remnant filter is given by [15]:

$$H_n(s) = K_n/\left(1+\tau_n s\right)^2 \tag{9}$$

with K_n the remnant gain and τ_n the remnant time constant (0.6 s) [5]. The remnant realisations were scaled such, that the remnant power *ratio* P_n, 10, remains consistent across all $3,000$ realizations. To do this, the remnant gain K_n is adjusted for each realization, to keep it within $\pm 1\%$ of the power ratio setting. P_n was set at 0.05, 0.1 or 0.2, with σ_n^2 the variance of the remnant and σ_u^2 the variance of the HC control input:

$$P_n = \sigma_n^2 / \sigma_u^2 \tag{10}$$

To maintain a constant remnant power ratio for both HCs, the remnant gain K_n of the high-gain HC needs to be larger. Note that, since $n(t)$ equals white noise $w(t)$ passed through the remnant filter $H_n(s)$, (2) shows that the innovation signal variance σ_η^2 is proportional to the remnant power ratio.

IV. Results

A. ROC curves

Figs. 5a-5c show the ROC curves ($\mathrm{TP_{rate}}$ vs. $\mathrm{FP_{rate}}$) for the innovation signal exceeding $\mathrm{C}\sigma_\eta$, for the low-gain, three remnant power ratios P_n, and observer gains K from 0.01 (dark green) to 0.9 (yellow). Note that the TP_{rate}s were generally very high, i.e., > 0.9. The HC gain (crossover frequency) had a negligible effect on these curves (not shown, see [16]); minor differences occur for higher P_n.

Lower observer gains result in fewer TPs and FPs for every threshold C. For very low observer gains, in the range of $0.01 - 0.1$, the integration of the remnant through the SI CE dynamics before transition causes the innovation signal to become slower and have a larger magnitude, i.e., the random walk. Higher observer gains lead to the opposite effect, and are preferred as they lead to good detection, especially when combined with larger C values. Higher K values result in more FPs per realisation for every C. However, since only one FP is counted per realisation , increased FPs *per realisation* do not impact the ROC curve. The higher frequency behavior of the innovation signal causes more FPs per realisation, but also a higher TP rate post-transition.

The choice of the threshold C has a relatively small impact on the TP and FP rates. Lower values, $\mathrm{C} \leq 2$, lead to more FPs, but also an increase in TP rate, resulting in almost always a detection for any observer gain, see Table II. The high FP rate means that the lower values of C are not desired for the detection of changes in CE dynamics. Higher values, $\mathrm{C} > 4$ cause very few FPs but also very few TPs, especially for lower observer gains K. Hence, for lower observer gains, $K < 0.1$, C must be between 2 and 3. For K around 0.1, C values between 3 and 4 are preferred. For higher K values, $K > 0.5$, C values between 4 and 5 are preferred.

TABLE II: TP and FP rates ($K_p = 5.5$, $P_n = 0.2$).

K (-)		C=1	C=2	C=3	C=4	C=5	C=6
0.01	$\mathrm{TP_{rate}}$	$\approx$1	0.95	0.89	0.80	0.71	0.49
	$\mathrm{FP_{rate}}$	0.49	0.01	0	0	0	0
0.1	$\mathrm{TP_{rate}}$	$\approx$1	$\approx$1	$\approx$1	0.98	0.97	0.94
	$\mathrm{FP_{rate}}$	1	0.55	0.04	0	0	0
0.5	$\mathrm{TP_{rate}}$	1	1	1	1	1	$\approx$1
	$\mathrm{FP_{rate}}$	1	$\approx$1	0.27	0.01	0	0
0.9	$\mathrm{TP_{rate}}$	1	1	1	1	$\approx$1	$\approx$1
	$\mathrm{FP_{rate}}$	1	$\approx$1	0.40	0.02	0	0

Finally, when remnant power ratio increases, the number of TPs decreases and the number of FPs increases, as expected. For all observer gain values, detection performance worsens. For larger observer gains, $K > 0.5$, effects of remnant power ratio are much smaller. For lower observer gains, higher remnant power ratios decrease the number of TPs and FPs as the relative effect of the target function on the innovation signal is smaller post-transition. The reduction in FPs is especially true for the larger analytical bounds σ_η. This means that for lower remnant power ratios, lower thresholds of C around 2-3 can be used for the detection of changes in CE dynamics.

B. Average detection times

Figs. 6a-6f show the average detection times for observer gains 0.01 to 0.9, both HC gains, three remnant power rations P_n, as a function of the threshold C. These also include the fastest, average and slowest HC detection times as experimentally obtained [5]. Similar to the ROC curves, HC gain seems to have almost no effect on detection time.

The detection time is smallest for the highest observer gains, increases somewhat with remnant power ratio, and increases with higher thresholds C. For the highest K values, $K > 0.8$, detection time increases linearly with C. When C increases, detection times increase more quickly for higher P_n. The high-gain HC detects earlier than the low-gain HC.

Table III is constructed using the ROC curves by considering the value of C that results in the lowest FP rate and highest TP rate. K ranges between 0.01 and 0.9, both low- and high-gain HCs are considered, and P_n is either 0.05, 0.1 or 0.2. C is between 2-3 for $K = 0.01$, between 3-4 for $K = 0.1$ and between 4-5 for $K = 0.9$.

TABLE III: Average detection times.

		average detection time (s)	
P_n	K (-)	$K_p = 3.5$	$K_p = 5.5$
0.05	0.01	$1.69 - 2.24$	$1.66 - 2.26$
	0.1	$1.09 - 1.30$	$1.06 - 1.27$
	0.5	$0.91 - 0.99$	$0.83 - 0.94$
	0.9	$0.76 - 0.86$	$0.73 - 0.85$
0.1	0.01	$2.18 - 2.99$	$2.21 - 3.00$
	0.1	$1.33 - 1.60$	$1.31 - 1.60$
	0.5	$1.06 - 1.22$	$1.01 - 1.15$
	0.9	$0.92 - 1.05$	$0.88 - 1.01$
0.2	0.01	$2.94 - 3.84$	$2.95 - 3.61$
	0.1	$1.73 - 2.11$	$1.73 - 2.17$
	0.5	$1.32 - 1.54$	$1.30 - 1.51$
	0.9	$1.16 - 1.32$	$1.09 - 1.28$

The table shows that the average detection time varies for the HC gain K_p: a higher K_p reduces the detection time, mainly because the HC control signal $u(t)$ has a larger amplitude. The remnant power ratio increases the detection time, mainly because of a reduced effect of the target function $f_t(t)$ on the post-transition innovation signal. Lower observer gains K cause a slower detection, mainly due to the low-frequency behavior of the innovation signal.

The table further shows that the detection *window*, i.e., the difference between the lower and upper limit of the average detection time, is much smaller for higher observer gains. For

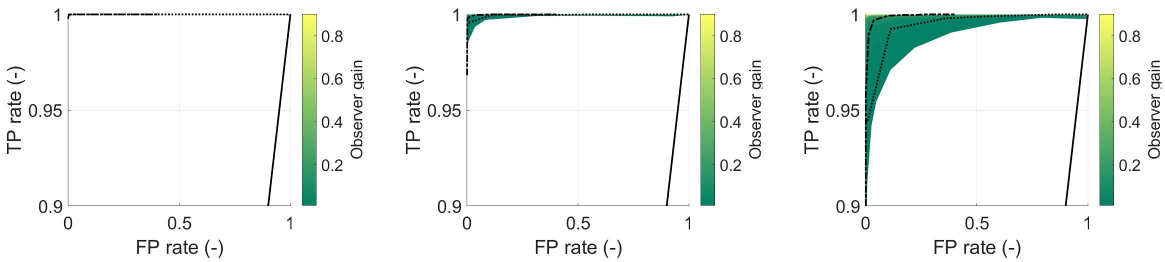

(a) $K_p = 3.5$, $P_n = 0.05$. (b) $K_p = 3.5$, $P_n = 0.1$. (c) $K_p = 3.5$, $P_n = 0.2$.

Fig. 5: ROC curves for low-gain HC, three remnant power ratios P_n, and observer gains K from 0.01 (dark green) to 0.9 (yellow). The dash dotted line and dotted line represent C=3 and C=2. Note that the y-axis runs from 0.9 to 1.

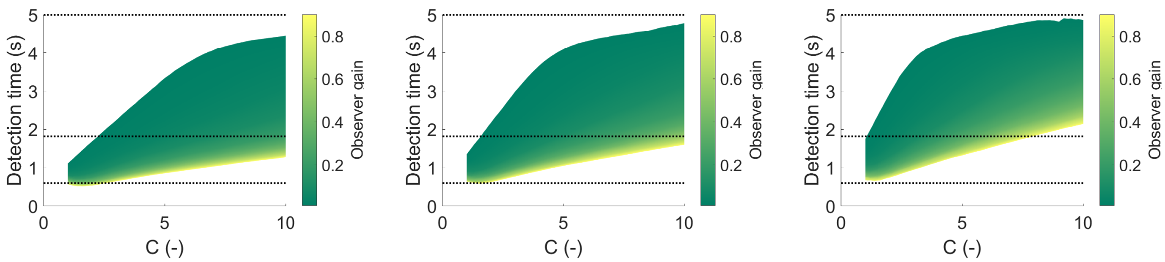

(a) $K_p = 3.5$, $P_n = 0.05$. (b) $K_p = 3.5$, $P_n = 0.1$. (c) $K_p = 3.5$, $P_n = 0.2$.

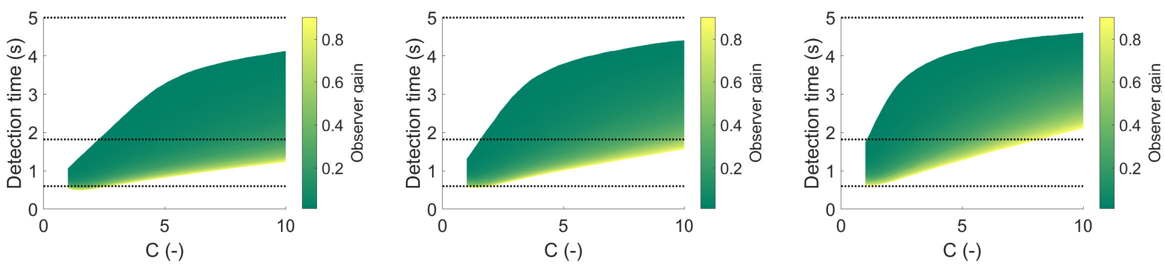

(d) $K_p = 5.5$, $P_n = 0.05$. (e) $K_p = 5.5$, $P_n = 0.1$. (f) $K_p = 5.5$, a $P_n = 0.2$.

Fig. 6: Average detection time versus C (from 1 to 10), for two HC gains, three remnant power ratios P_n, three HC gains and observer gains K from 0.01 to 0.9. Horizontal lines show the fastest, average and slowest detection times from [5].

$K = 0.9$ the detection window is between 0.1 s ($P_n = 0.05$) and 0.2 s ($P_n = 0.2$). For $K = 0.01$, the detection window for these remnant power ratios is 0.5 and 0.9 s, respectively.

Note that the predicted detection time does not include any human reaction time delays. Nonetheless, the average detection times match the experimentally observed detection times from [5] extremely well, indicating that the proposed model has potential to characterize and predict human detection times when confronted with changing CE dynamics in a pursuit tracking task.

V. Discussion

The MC simulation results show that effects of HC gain are negligible, which implies that the proposed model performs well for more and less aggressive controllers. In addition, the same threshold levels C can be used. Detection times were approximately equal for the low- and high-gain HCs, which corresponds well with experimental data [5].

In our model, *before* a CE transition the HC's internal model $H^*_{CE}(s)$ matches the CE dynamics $H_{CE}(s)$ and the innovation signal $\eta(t)$ is only affected by HC remnant. Higher remnant power ratios result in (proportionally) larger innovation signal variances, causing higher thresholds C to accurately detect changes in CE dynamics and slower detection of the change in CE dynamics. This matches common sense very well, e.g., a tired or inattentive HC would control with higher remnant levels, and to avoid too many false positives the detection threshold must be raised, slowing down detection. *After* CE transition, the innovation signal is also affected by the target signal $f_t(t)$, see (1). For lower P_n, this effect is larger, causing the thresholds to be exceeded more quickly and detection times to decrease, Table III.

The detection threshold C must be set to minimize false positives *before* CE transition, and maximize true positives *after* transition. Previous research showed that for compensatory tracking, a detection threshold of $\approx$3.9 on either error $e(t)$ or error-rate $\dot{e}(t)$ worked well [10]. For pursuit tracking, experimental data revealed thresholds between 3.6-4 on $\dot{y}(t)$, the CE output [5]. While working on different signals, these thresholds correspond well with the C levels found in our

MC analysis, which depended on the observer gain K. For $0.01 < K < 0.1$ a threshold of 2-3σ_η, for $0.1 < K < 0.5$ 3-4σ_η and for $0.5 < K < 0.9$ 4-5σ_η is proposed. These C levels suggest that HCs typically employ a relatively high detection threshold: three to four times the standard deviation of the signal being monitored for detection.

The detection time depends on the observer gain K: it decreases for larger gains K, see Table III. Note that this detection time excludes any human reaction times, which are typically ≈200 ms [2]. The experimentally-determined detection times, for the same control task settings as investigated here, varied between 0.6 and 5 seconds, on average 1.82 seconds [5]. Subtracting the reaction time leads to an average detection time comparable to our MC simulations of 1.62 s. The settings of our model, tuned for the experimental data of Barragan et al. [5], would be as follows. For a remnant power ratio of 0.2, K between 0.1-0.4 and C values in the range 3-4, detection times between 1.30 and 2.11 s are found, which correspond well with [5].

In the experiment of Barragan et al. [5], with 17 participants and six trials per participant, two false positives were made, a false positive rate of $2/102 \approx 0.02$. No false negatives were recorded. These findings also correspond well with the results obtained from our HC observer model.

There are multiple avenues for future research. First, whereas in our model we assume the HC to perform almost perfectly linearly in steady-state, it could well be that in reality a (clever) HC would sometimes introduce 'test inputs', some arbitrary stick movement to excite the CE. In this case, the HC might be able to detect a change in CE dynamics more quickly, i.e., exploiting the innovation signal $\eta(t)$ [4]. This would be an effective strategy, as in reality HCs' internal CE dynamics model will likeluy never perfectly match the actual CE dynamics, and is also a crucial future research direction for extending the model to incorporate the *identification* and *modification* phases [2]. Hence, the proposed observer model and this hypothesized 'probing' strategy can be further validated using experiments with different CE dynamics and CE transitions. Secondly, perhaps the derivative of the innovation signal, $\dot{\eta}(t)$, may play a role in detecting changes in CE dynamics. Previous research indicated that 'rate-of-change' of some monitored variable, like $\dot{e}(t)$ in compensatory tasks, or $\dot{y}(t)$ in pursuit, can be useful [2], [4], [5], [8], [13], [17].

The internal model hypothesis has been fundamental in research on changes in CE dynamics [8], [9], [12], [18]. It has never been analyzed for pursuit-tracking tasks, however, [4], and this study provided some pioneering results. The innovation signal seems to provide a potential basis for predicting how and when humans detect changes in CE dynamics. Our model, unlike MRAC [12] or detection methods based on $y(t)$, $\ddot{y}(t)$ [5], $e(t)$ or $\dot{e}(t)$ [10], does not need a lot of reference data. It can predict the moment a HC detects a change in CE dynamics well and only uses the HC control signal $u(t)$ and, crucially, enables incorporating effects of HC 'probing' whether a change in CE dynamics occurred by using a test input, which the other models do not allow.

VI. Conclusions

The proposed model shows promise for modeling human detection of changes in CE dynamics. While the HC gain had a negligible effect, increasing remnant power ratios led to decreasing true *and* false positive rates. This is because, with more remnant, the target signal contribution to the innovation signal reduces. Observer gains of 0.1-0.5, with thresholds of 3σ-4σ, compared well with previous studies, resulted in high true positive and low false positive rates, and led to average detection times that closely match experimental HC data.

References

[1] W. Plaetinck, D. M. Pool, M. M. Van Paassen, and M. Mulder, "Online Time-Varying Identification and Detection of Pilot Adaptation with Recursive ARX Models," *J. of Guidance, Control & Dynamics*, vol. 48, no. 5, p. 1112–1123, 2025.

[2] L. R. Young, "On Adaptive Manual Control," *IEEE Transactions on Man-Machine Systems*, vol. 10, no. 4, pp. 292–331, 1969.

[3] P. M. T. Zaal, "Manual Control Adaptation to Changing Vehicle Dynamics in Roll–Pitch Control Tasks," *J. of Guidance, Control, and Dynamics*, vol. 39, no. 5, pp. 1046–1058, 2016.

[4] M. Mulder, D. M. Pool, K. Van der El, and M. M. Van Paassen, "Neuroscience Perspectives on Adaptive Manual Control with Pursuit Displays," in *15th IFAC-HMS Symposium, San Jose (CA), USA*, 2022, pp. 160–165.

[5] M. Barragan, D. M. Pool, M. M. Van Paassen, and M. Mulder, "Predicting Human Operators' Detection of Time-Varying Changes in Controlled Element Dynamics," in *AIAA Modeling and Simulation Technologies Conf.*, no. AIAA-2025-0974, 2025.

[6] P. D. Neilson and M. D. Neilson, "A Neuroengineering Solution to the Optimal Tracking Problem," *Human Movement Science*, vol. 18, pp. 155–183, 1999.

[7] P. D. Neilson, M. D. Neilson, and N. J. O'Dwyer, "Adaptive Optimal Control of Human Tracking," in *Motor Control and Sensory Motor Integr.: Issues and Directions*, I. D. J. Glencross and J. P. Piek, Eds. Elsevier, 1995, p. 97–140.

[8] D. C. Miller and J. I. Elkind, "The Adaptive Response of the Human Controller to Sudden Changes in Controlled Process Dynamics," *IEEE Trans. on Hum. Fact. in Electr.*, vol. 8, no. 3, pp. 218–223, 1967.

[9] A. V. Phatak and G. A. Bekey, "Decision Processes in the Adaptive Behavior of Human Controllers," *IEEE Trans. on Systems Science and Cybernetics*, vol. 5, no. 4, p. 339–351, 1969.

[10] J. Van Ham, D. M. Pool, and M. Mulder, "Predicting Human Control Adaptation from Statistical Variations in Tracking Error and Error Rate," in *15th IFAC-HMS Symposium, San Jose (CA), USA*, 2022, pp. 166–171.

[11] R. Hess, "Modeling Pilot Control Behavior with Sudden Changes in Vehicle Dynamics," *J. of Aircraft*, vol. 46, pp. 1584–1592, 09 2009.

[12] L. Terenzi, P. M. T. Zaal, D. M. Pool, and M. Mulder, "Adaptive Manual Control: a Predictive Coding Approach," in *AIAA Modeling and Simulation Technologies Conf.*, no. AIAA-2022-2448, 2022.

[13] D. T. McRuer and H. R. Jex, "A Review of Quasi-Linear Pilot Models," *IEEE Trans. on Human Factors in Electronics*, vol. 8, no. 3, pp. 231–249, 1967.

[14] E. K. Vinodh, J. Jovitha, and S. Ayyappan, "Comparison of Four State Observer Design Algorithms for MIMO Systems," *Arch. of Control Sciences*, vol. 23, no. 2, pp. 243–256, 2013.

[15] K. Van der El, D. M. Pool, M. M. Van Paassen, and M. Mulder, "Analysis of Human Remnant in Pursuit and Preview Tracking Tasks," in *14th IFAC HMS Symposium, Tallinn, Estonia*, 2019, pp. 145–150.

[16] T. Eppenga, "Predicting Detection of Changes in Controlled Element Dynamics by Human Controllers' Internal Model," Master's thesis, TU Delft, 2024.

[17] M. Mulder, D. M. Pool, D. A. Abbink, E. R. Boer, P. M. T. Zaal, F. M. Drop, K. van der El, and M. M. van Paassen, "Manual Control Cybernetics: State-of-the-Art and Current Trends," *IEEE Trans. on Human-Machine Systems*, vol. 48, no. 5, pp. 468–485, 2018.

[18] R. Hess, "Modeling the Pilot Detection of Time-Varying Aircraft Dynamics," *Journal of Aircraft*, vol. 49, pp. 2100–2104, 11 2012.